



Demonstrate the Out-of-Pile Performance of a Real-time Measurement System to Measure Thermal Conductivity Based on Photo Thermal Radiometry

May 2021

Zilong Hua
Robert Schley



*INL is a U.S. Department of Energy National Laboratory
operated by Batelle Energy Alliance, LLC*

DISCLAIMER

This information was prepared as an account of work sponsored by an agency of the U.S. Government. Neither the U.S. Government nor any agency thereof, nor any of their employees, makes any warranty, expressed or implied, or assumes any legal liability or responsibility for the accuracy, completeness, or usefulness, of any information, apparatus, product, or process disclosed, or represents that its use would not infringe privately owned rights. References herein to any specific commercial product, process, or service by trade name, trade mark, manufacturer, or otherwise, does not necessarily constitute or imply its endorsement, recommendation, or favoring by the U.S. Government or any agency thereof. The views and opinions of authors expressed herein do not necessarily state or reflect those of the U.S. Government or any agency thereof.

Demonstrate the Out-of-Pile Performance of a Real-time Measurement System to Measure Thermal Conductivity Based on Photo Thermal Radiometry

**Zilong Hua
Robert Schley**

May 2021

**Idaho National Laboratory
Idaho Falls, Idaho 83415**

<http://www.inl.gov>

**Prepared for the
U.S. Department of Energy
Office of Nuclear Energy
Under DOE Idaho Operations Office
Contract DE-AC07-05ID14517**

Page intentionally left blank

SUMMARY

The goal of this project is to develop a fiber-based instrument to perform in-reactor thermal conductivity measurements of fuels and materials. This instrument is based on photothermal radiometry (PTR) and involves heating a sample locally and measuring the induced temperature gradient by collecting blackbody radiation [2]. Thermal conductivity of the sample is extracted by comparing experimental results with a continuum-based model [3,4]. As a laser-based technique, PTR is a non-contact measurement technique that can be performed remotely and non-destructively. In addition, it has several advantages over other photothermal techniques, making it an ideal approach for in-situ measurement of thermal conductivity of nuclear fuels. Because blackbody radiation increases with emissivity and temperature, the PTR technique works well with unprepared surfaces, and measurement accuracy increases with temperature. Moreover, this approach is capable of measuring samples with irregular or poorly defined boundary conditions, which is a common situation for friable spent fuels.

Page intentionally left blank

CONTENTS

SUMMARY.....	iii
ACRONYMS.....	vii
1. INTRODUCTION.....	1
2. DEVELOPMENT AND FABRICATION OF THE INSTRUMENT.....	1
3. TESTING RESULTS.....	3
4. DISCUSSION.....	5
5. SUMMARY AND PATH FORWARD.....	6
6. REFERENCES.....	6

FIGURES

Figure 1 (Left) a photo of the vacuum chamber with the instrument and sample inside; (right) a close-up photo of the instrument probe approaching the sample surface.....	2
Figure 2 The design diagram of the experimental setup.....	3
Figure 3 Experimental data and fitted results of Al ₂ O ₃ at four temperature points.....	4
Figure 4 Measured thermal diffusivity with respect to temperature of all reference samples.....	5

Page intentionally left blank

ACRONYMS

DOE	Department of Energy
FY	fiscal year
IR	infrared
PIE	post-irradiation examination
PTR	photothermal radiometry

Page intentionally left blank

Demonstrate the Out-of-Pile Performance of a Real-time Measurement System to Measure Thermal Conductivity Based on Photo Thermal Radiometry

1. INTRODUCTION

Thermal conductivity of nuclear fuels and related materials is a central physical property governing fuel behavior under irradiation (e.g., swelling, fission gas transport, safety margins). Microstructure defects (e.g., point defects, dislocation loops, small defect clusters) are generated and continuously evolve during the reactor operation, which result in reduction of the thermal conductivity[1]. Understanding how thermal conductivity changes with irradiation is critical for high burnup fuels, and is also key in developing advanced fuels with high conductivity. Currently, the experimental validation of thermal property related studies relies on post-irradiation examination (PIE). However, researchers have speculated for years that the actual conductivity during irradiation can be significantly smaller than that measured through PIE. The reason for this is that point defects, which effectively scatter thermal carriers, anneal before PIE measurements can be performed. An instrument that enables accurate, in-reactor measurements of fuel conductivity will enable validation of new, advanced fuel performance codes.

The goal of this project is to develop a fiber-based instrument to perform in-reactor thermal conductivity measurements of fuels and materials. This instrument is based on photothermal radiometry (PTR) and involves heating a sample locally and measuring the induced temperature gradient by collecting blackbody radiation [2]. Thermal conductivity of the sample is extracted by comparing experimental results with a continuum-based model [3,4]. As a laser-based technique, PTR is a non-contact measurement technique that can be performed remotely and non-destructively. In addition, it has several advantages over other photothermal techniques, making it an ideal approach for in-situ measurement of thermal conductivity of nuclear fuels. Because blackbody radiation increases with emissivity and temperature, the PTR technique works well with unprepared surfaces, and measurement accuracy increases with temperature. Moreover, this approach is capable of measuring samples with irregular or poorly defined boundary conditions, which is a common situation for friable spent fuels.

In this report, we will first briefly review the development and fabrication of the prototype (first-generation) and upgraded (second-generation) instruments (Section 2). During this fiscal year (FY21), a vacuum chamber has been procured and used for high temperature, in-situ measurements. The details will also be given in Section 2. In Section 3, measurements on reference materials taken in the vacuum chamber which simulate real-time, in-situ thermal diffusivity measurements are presented. Thermal diffusivity can be converted to conductivity with known density and heat capacity. The conductivity of these samples covers a range typical of spent oxide fuels to fresh metallic fuels. The measurement uncertainty, possible experimental errors, and possibilities for optimization are discussed in Section 4. The feasibility assessment for conducting in-reactor measurements and a path forward for achieving this goal are presented in Section 5. More technical details of the PTR system (e.g., the physics model of thermal wave generation and propagation, the mathematical heat conduction model, and the roles that each component plays in the system, etc.) can be found in previous milestone reports (INL/EXT-19-53710, INL/INT-20-58303, and INL/EXT-20-59955).

2. DEVELOPMENT AND FABRICATION OF THE INSTRUMENT

Development of an optical fiber-based PTR instrument began in FY20. An initial probe (first-generation) was developed with the target to validate the probe design by performing room temperature measurements. Fibers and detectors working in the mid to long infrared (IR) wavelength range were used for the first-generation probe. InF₃ fibers were selected for IR radiation collection, which had a usable transmission wavelength in the 0.5–5 μm range but had a maximum service temperature of only 90°C. Work with this probe and the associated liquid nitrogen filled detector was presented in the FY20 mid-year status report (INL/INT-20-58303). The conclusion from testing the first-generation

instrument was that the optical fibers and detector should be matched for a particular IR wavelength range and corresponding temperature range (based on the Planck radiation curve). Based on this conclusion, a second-generation probe was developed which was optimized for performing measurements in the temperature range of reactor environments. This probe used gold coated silica fiber along with a Thorlabs PDA10DT detector optimized for the 1 to 2.5 μm wavelength range. The gold coated silica fiber is much more robust than the InF_3 fiber and has a maximum operating temperature of about 700°C. The downside to the probe incorporating the silica fiber was that a usable signal is not available until the sample reaches 250 to 300°C due to the shorter wavelength transmission range. Initial results using this probe were reported in the FY20 yearend report (INL/EXT-20-59955).

Continued testing in FY21 revealed limitations in the sample heating methodology and the experiment configuration. Sample heating consisted of a horizontal aluminum bar with sample pocket machined in one end. A cartridge heater mounted in the aluminum bar provided the heat source. The sample was placed in the sample pocket, and the probe and thermocouple measurements were made on the vertical sample surface. The entire sample heater was placed on a hot plate to aid in reaching higher temperatures. The maximum temperature obtained on an alumina sample was about 495°C. However, the experiment configuration tended to increase the effects of convective heat transfer, and the graphite coating used on the sample oxidized in the air environment and was completely gone by the end of the test [5]. It was determined that an improved setup was required for effective probe testing.

A small vacuum chamber was procured to allow testing to be performed without the effects of convective heat transfer and to minimize oxidation at high temperatures. A new vertical sample holder was designed with a ceramic base to minimize conduction to the vacuum chamber walls. The probe was also configured in a vertical position and was supported using a bushing which allowed the probe to slide to prevent stresses due to thermal expansion mismatch. Probe contact with the sample was due solely to the weight of the probe. A new probe which incorporated a vacuum feedthrough was designed and fabricated. Construction of the probe was the same as that reported in the FY20 yearend report, and the fiber separation was again approximately 171 μm . A photo of the vacuum chamber and a closeup of the probe and sample are shown in Figure 1, and a diagram of the experimental setup is shown in Figure 2. Using the new vacuum chamber, experiment setup testing measurements were made on several reference samples. Temperatures over 500°C were easily obtained with no oxidation issues, and the data, reported in the next section, better matches the continuum model than tests using the previous setup.

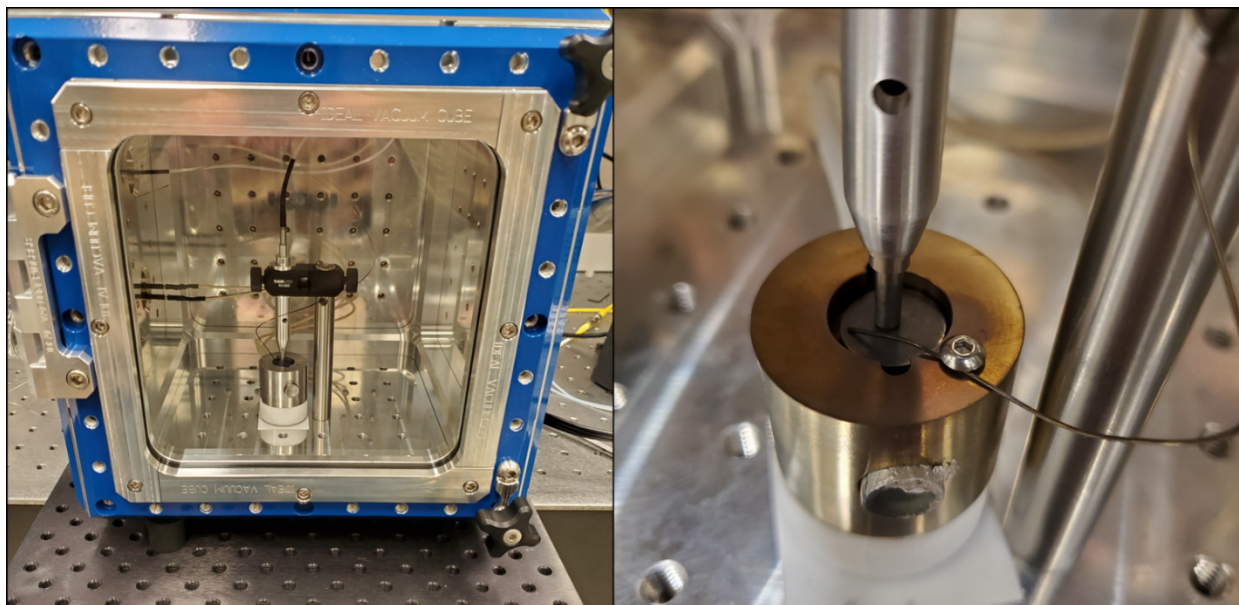


Figure 1 (Left) a photo of the vacuum chamber with the instrument and sample inside; (right) a close-up photo of the instrument probe approaching the sample surface.

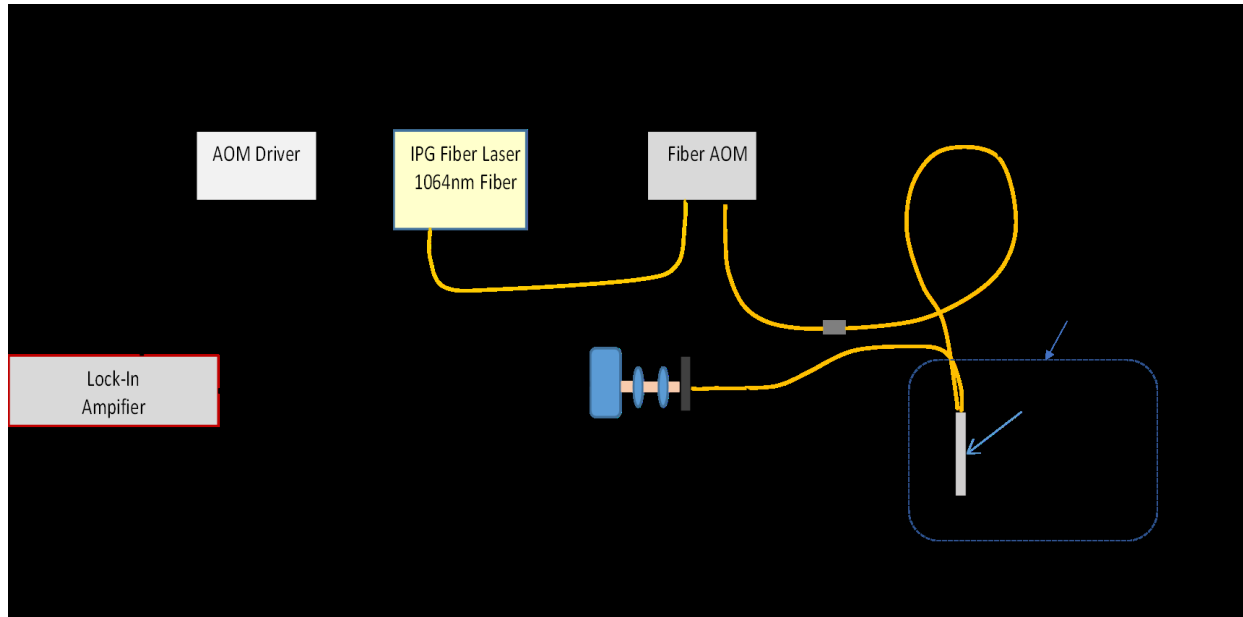


Figure 2 The design diagram of the experimental setup.

3. TESTING RESULTS

In-situ thermal diffusivity measurements were performed on a set of reference materials, Pyrex, pyroceram, alumina, and poco graphite (with the order of lowest thermal diffusivity at room temperature to highest), in the temperature range of $\sim 240^{\circ}\text{C}$ to 520°C . At room temperature, their thermal diffusivity values cover a wide range of $<1\text{mm}^2/\text{s}$ to $65\text{mm}^2/\text{s}$, containing the common values of fresh metallic fuels to spent oxide fuels. The thermal wave phases were recorded over the frequency range of 1Hz to 2000Hz, and thermal diffusivity was extracted by fitting the experimental data to the model prediction in a specific frequency window. The starting frequency window was preset based on the thermal diffusivity of common materials, and a threshold of minimum thermal wave amplitude. The window is then adjusted by an iterative fitting program, so that the thermal diffusion length, calculated from the best-fit thermal diffusivity in the last iteration, is not too long compared to the sample thickness, or too short compared to the diffraction pattern radius. The details of this criterion and the related physics can be found in our previous milestone report.

The measurement results are summarized and plotted in [Figure 3](#) and [Figure 4](#). In Figure 3, data from measurements of Al_2O_3 are used as an example to show raw data of the in-situ measurements (blue and red stars), and how the data compare to the calculation from the continuum model (dark dash lines). Note the blue stars were excluded from the fitting process because these data points were influenced by the rear surface of the sample due to the long diffusion length at these frequencies. As can be seen in [Figure 3](#), the phase measurement uncertainty significantly decreases with temperature, indicating a higher signal to noise ratio. This matches our expectation that blackbody radiation heat flux increases with temperature. It should also be noted that the extracted thermal diffusivity decreases with temperature, which is expected for oxide materials that have phonons as the primary thermal carriers [6].

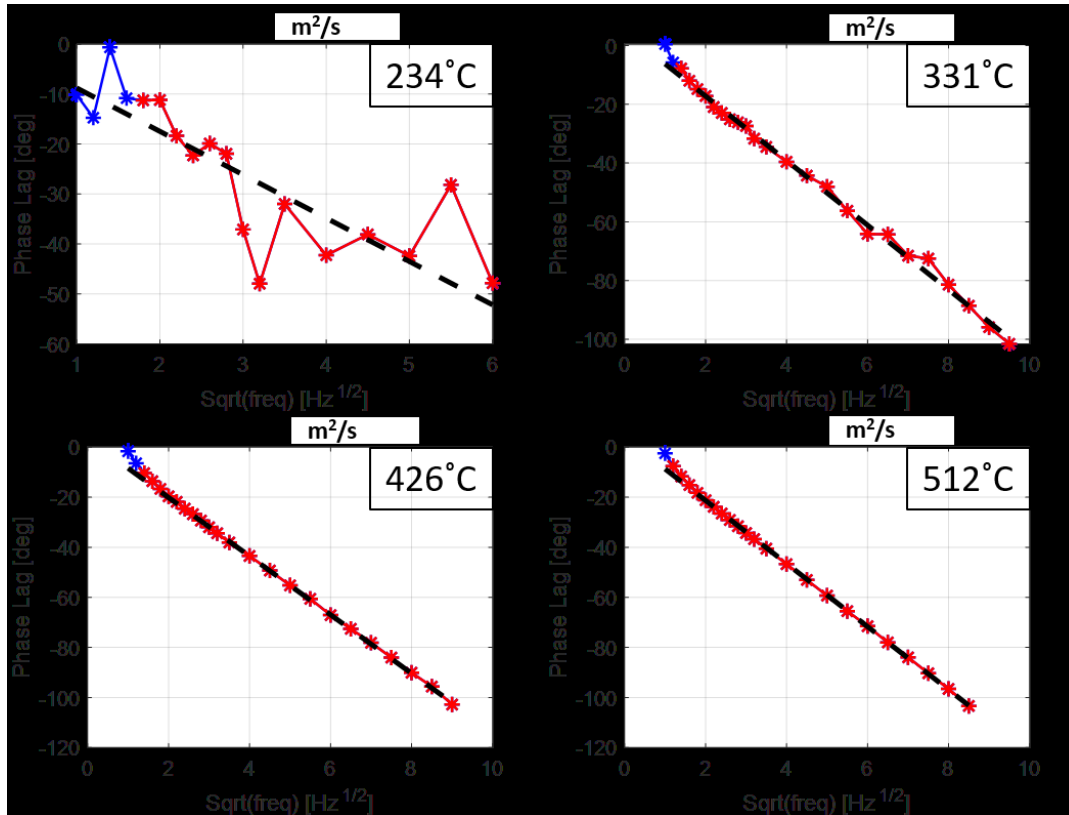


Figure 3 Experimental data and fitted results of Al₂O₃ at four temperature points. Experimental data are given in stars, with the blue ones excluded from the fitting process. The fitting curves are given in dark dash lines, and the best-fit thermal diffusivity values are given in the title.

The thermal diffusivity values with respect to measurement temperature are plotted in [Figure 4](#) for all reference samples (red stars), with the literature values given (dark solid lines) as the validation of the measurement approach and the instrument [7-10]. Measured thermal diffusivity values agree well with the literature values on the two thermally slower materials. For Pyrex above 300°C and for pyroceram above ~380°C, the differences of measured values and literature values are approximately 10%. The large error in the “low” temperature range is primarily due to the significantly lower signal to noise ratio. For thermally faster materials Al₂O₃ and poco graphite, the differences between the measured thermal diffusivity values and literature values are slightly larger, but still generally smaller than 25%. Additionally, the results in the “low” frequency range are more consistent, compared to the results of the slower materials. The main reason is that for thermally faster materials, the thermal wave amplitude decreases less with respect to frequency, and, as a result, the data in a wider frequency window can be used in the fitting process. For instance, thermal diffusivity of Pyrex at 269°C is determined only by data points from 1-6Hz, while alumina at 234°C is determined by data points from 4-35Hz. Overall, the new instrument shows the capability of accurately measuring thermal diffusivity of all reference materials above 350°C.

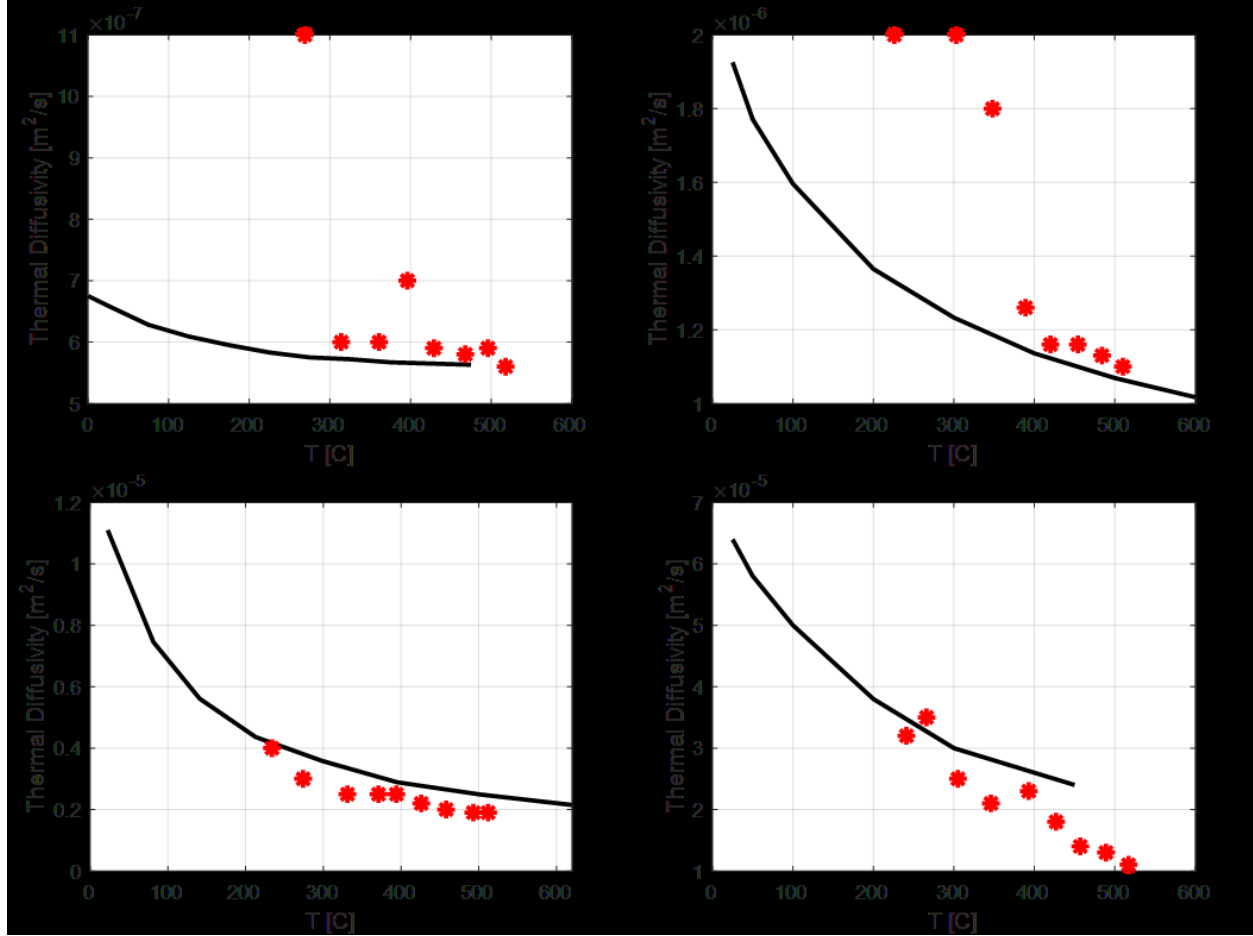


Figure 4 Measured thermal diffusivity with respect to temperature of all reference samples. The experimental data are given in red stars, and the literature values are given in the dark line.

4. DISCUSSION

Two topics important for the future real-time, in-reactor measurements will be discussed in this section: how to improve the measurement accuracy and speed. To improve the measurement accuracy, it is important to know where the experimental uncertainty and errors are from, and how to reduce them. The experimental uncertainty is inversely related to the signal-to-noise ratio. The results shown earlier have validated our statement that the signal level and, thus, signal-to-noise ratio of this PTR-based instrument increases with temperature. Data with reasonably high signal amplitude can be obtained above 350°C on all reference materials. Considering that most reactors operate above this temperature, the experimental uncertainty issue is expected to be less of an issue in an actual in-situ scenario. At the (relatively) low temperature end, we have also noticed that the uncertainty can be reduced by using a longer time constant and increasing the frequency sampling rate.

As indicated by the lines representing literature values in [Figure 4](#), the thermal diffusivity of all samples shows a strong dependence on temperature. Consequently, an experimental error can be introduced if the sample temperature is not accurately measured, and the precision of the thermocouple-measured temperature needs to be confirmed. Our measurements correctly captured the variation trends of thermal diffusivity with respect to temperature on all sample materials, but all curves are apparently shifted from the literature values. In order to confirm the measurement temperature, we borrowed a high-end pyrometer from our colleague. Unfortunately, the pyrometer would not work through the window of the vacuum chamber. We plan to perform the measurements without using the

vacuum chamber to confirm the temperature. If a deviation exists in the actual temperature vs the thermocouple indicated temperature, we will look for a better bonding approach to improve the contact coupling condition of the thermocouple and the sample surface or possibly create a heat shield to reduce the thermal gradient.

Assuming the deviation of the temperature read by the thermocouple is not significant enough to cause the differences in [Figure 4](#), we can see two possible probe related sources of the error. The first source is an insufficient offset distance between the heating and detection fibers. As we discussed in the previous milestone report [11], the ratio of the offset distance and the convolved heating/probe spot size needs to be larger than five. Although this ratio is achieved during the instrument fabrication, the distance between the fiber head and the sample surface may equivalently increase the convolved spot size and, thus, reduce this ratio. We plan to examine this effect by performing the measurements with different fiber-to-sample distances. If needed, a new instrument with a larger offset distance will be fabricated and tested. The second source is from the PTR technique. As we discussed in the previous milestone report, the diffraction and nonlinearity issues are found on the free-space PTR system, which may lead to systematic overestimation of thermal diffusivity [12]. As these issues are more common on materials with low thermal diffusivity, it may explain the higher measured thermal diffusivity on Pyrex and pyroceram. Diffraction and nonlinearity issues are known to be worse at high frequency and with high modulation amplitude of the heating laser, we will change the modulation of the heating laser and the frequency window in the fitting process to better explore this.

All the results included in this report were obtained and analyzed in a real-time manner. Currently, it takes 10-15 minutes to collect the data (sweep the modulation frequency from 1Hz to 2000Hz), and 10-15 seconds to finish the fitting process. Therefore, the data collection is the bottleneck of the measurement speed. Our data collection approach is designed for “blind” measurements that have no knowledge of the sample thermal diffusivity a priori. This is the reason why an unnecessarily large modulation frequency range is used. As a matter of fact, only a small fraction of collected phase data are used in the fitting process to determine the thermal diffusivity (e.g., 4-35Hz for alumina at 234°C). It is possible to improve the data collection speed by decreasing this frequency range, if thermal diffusivity of the sample material can be estimated, for instance, from a preliminary test or from literature. Furthermore, the curve of the phase lag- $f^{1/2}$ is expected to be linear. As shown in [Figure 3](#), when the signal amplitude is high at high temperatures, a sufficient accuracy is achievable by performing measurements in a much narrower frequency window (e.g., 30-50Hz at 512°C) and with few data spots. This could significantly reduce the time needed for the data collection.

5. SUMMARY AND PATH FORWARD

In this report, the recent progress in the development of fiber-based PTR instrument for in-reactor, real-time thermal conductivity measurements is summarized. The in-situ testing has been performed on four reference samples with thermal transport properties covering the range from fresh metallic fuels to spent oxide fuels. Tests were conducted in the temperature range of ~240°C - ~520°C in a vacuum chamber. Good accuracy is obtained on all samples above 350°C, due to significantly higher radiation heat flux signal resulting in an improved signal to noise ratio. The technical readiness level of this instrument is further improved, and we are another step closer to the final deployment stage of in-reactor tests.

Possible optimization to improve the measurement accuracy and speed have been discussed, and accordingly, an experimental plan has been made. In addition to the optimization discussed in Section 4, we also plan to increase the experiment temperature to test the fiber survivability, and perform tests on more reference samples with the temperature dependence of thermal conductivity and diffusivity better defined.

6. REFERENCES

1. Snead, L., T. Burchell, “Thermal conductivity degradation of graphites due to neutron irradiation at low temperature,” *Journal of Nuclear Materials*, vol. 224, no. 3, pp: 222-229, (1995).

[https://doi.org/10.1016/0022-3115\(95\)00071-2](https://doi.org/10.1016/0022-3115(95)00071-2).

2. Fabbri, L., P. Fenici, "Three-dimensional photothermal radiometry for the determination of the thermal diffusivity of solids," *Review of Scientific Instruments*, vol. 66, no. 6, pp. 3593-3600 (1995). <https://doi.org/10.1063/1.1146443>.
3. Maznev, A., J. Hartmann, M. Reichling, "Thermal wave propagation in thin films on substrates," *Journal of Applied Physics*, vol. 78, no. 9, pp. 5266-5269, (1995). <https://doi.org/10.1063/1.359702>.
4. Hua, Z., H. Ban, M. Khafizov, R. Schley, R. Kennedy, D.H. Hurley, "Spatially localized measurement of thermal conductivity using a hybrid photothermal technique," *Journal of Applied Physics*, vol. 111, no. 10, pp. 103505 (2012). <https://doi.org/10.1063/1.4716474>.
5. Zhou, X., C.I. Contescu, X. Zhao, Z. Lu, J. Zhang, Y. Katoh, Y. Wang, B. Liu, Y. Tang, C. Tang, "Oxidation behavior of matrix graphite and its effect on compressive strength," *Science and Technology of Nuclear Installations*, vol. 2017, article 4275375 (2017). <https://doi.org/10.1155/2017/4275375>.
6. Berman, R., *Thermal Conduction in Solids*, Clarendon Press 1976.
7. Campbell, R.C., I.A. Beta, M.G. Manuelian, "Thermophysical Properties of Pyrex 7740 Glass Over the Temperature Range of -180°C to 475°C, *Thermal Conductivity 31/Thermal Expansion 19*, p.138, (2013).
8. Salmon, D., R. Brandt, R. Tye, "Pyroceram 9606, A Certified Ceramic Reference Material for High-Temperature Thermal Transport Properties: Part 2—Certification Measurements," *International Journal of Thermophysics*, vol. 31, no. 2, pp. 355-373 (2010). <https://doi.org/10.1007/s10765-010-0710-3>.
9. Hofmeister, A.M., "Thermal diffusivity and thermal conductivity of single-crystal MgO and Al₂ O₃ and related compounds as a function of temperature," *Physics and Chemistry of Minerals*, vol. 41, pp. 361-371, (2014). <https://doi.org/10.1007/s00269-014-0655-3>.
10. Min, S., J. Blumm, A. Lindemann, "A new laser flash system for measurement of the thermophysical properties," *Thermochimica Acta*, vol. 455, no. 1-2, pp. 46-49, (2007). <https://doi.org/10.1016/j.tca.2006.11.026>.
11. Hua, Z., H. Ban, D.H. Hurley, "The study of frequency-scan photothermal reflectance technique for thermal diffusivity measurement," *Review of Scientific Instruments*, vol. 86, no. 5, pp. 054901 (2015). <https://doi.org/10.1063/1.4919609>.
12. Bisson, J., D. Fournier, "The coupled influence of sample heating and diffraction on thermal diffusivity estimate with infrared photothermal microscopy," *Journal of Applied Physics*, vol. 84, no. 1, pp. 38-43 (1998). <https://doi.org/10.1063/1.367999>.